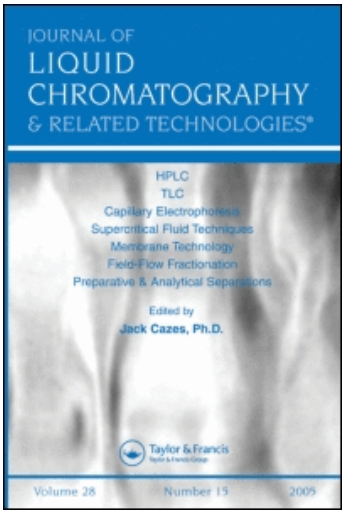

Journal of Liquid Chromatography & Related Technologies
Publication details, including instructions for authors and subscription information:
http://www.informaworld.com/smpp/title~content=t713597273

MICRO-CHANNEL THERMAL FIELD-FLOW FRACTIONATION: ANALYSIS OF ULTRA-HIGH MOLAR MASS POLYMERS AND COLLOIDAL PARTICLES WITH CONSTANT AND PROGRAMMED FIELD FORCE OPERATION

Josef Janca[a]
[a] Pôle Sciences et Technologie, Université de La Rochelle, La Rochelle, France

Online publication date: 28 August 2002

To cite this Article Janca, Josef(2002) 'MICRO-CHANNEL THERMAL FIELD-FLOW FRACTIONATION: ANALYSIS OF ULTRA-HIGH MOLAR MASS POLYMERS AND COLLOIDAL PARTICLES WITH CONSTANT AND PROGRAMMED FIELD FORCE OPERATION', Journal of Liquid Chromatography & Related Technologies, 25: 13, 2173 — 2191
To link to this Article: DOI: 10.1081/JLC-120014000
URL: http://dx.doi.org/10.1081/JLC-120014000

MARCEL DEKKER, INC. • 270 MADISON AVENUE • NEW YORK, NY 10016

JOURNAL OF LIQUID CHROMATOGRAPHY & RELATED TECHNOLOGIES
Vol. 25, Nos. 13–15, pp. 2173–2191, 2002

MICRO-CHANNEL THERMAL FIELD-FLOW FRACTIONATION: ANALYSIS OF ULTRA-HIGH MOLAR MASS POLYMERS AND COLLOIDAL PARTICLES WITH CONSTANT AND PROGRAMMED FIELD FORCE OPERATION

Josef Janca

Université de La Rochelle, Pôle Sciences et Technologie,
Avenue Michel Crepeau, 17042 La Rochelle Cedex 01,
France
E-mail: jjanca@univ-lr.fr

ABSTRACT

Separation and analysis of ultra-high molar mass (UHMM) polystyrenes by micro-Thermal Field-Flow Fractionation (μ-TFFF) was found to be very efficient in the range of molar masses over one million grams per mol. Although, constant field force operation allows achieving very high resolution, the programming of the temperature gradient is an advantageous operational mode from the point of view of the time of analysis. The programming, as well as the substantial extension of the perfectly controlled temperature of the cold wall, is much easier with the μ-TFFF channel due to an important decrease of the heat energy flux compared

DOI: 10.1081/JLC-120014000
1082-6076 (Print); 1520-572X (Online)

MARCEL DEKKER, INC. • 270 MADISON AVENUE • NEW YORK, NY 10016

with standard size channels. An example of the high performance analysis of colloidal particles by the μ-TFFF is presented.

Key Words: Micro thermal field-flow fractionation; Temperature gradient programming; Ultra-high molar mass polymers; Colloidal particles

INTRODUCTION

Separation and analysis of UHMM polymers represents a difficult task. The performance of the most currently used separation method, Size Exclusion Chromatography (SEC), which is very efficient within the range of molar masses from a few thousands up to roughly one million grams per mole is substantially reduced whenever the separation of UHMM polymers (over one million g/mole) is concerned. The separation and characterization of colloidal particles by the SEC is, at least, problematic. On the other hand, the thermal field-flow fractionation (TFFF) of polymers and even of colloidal particles has already been confirmed[1,2] as a very convenient method, applicable for the determination of the molar mass distribution (MMD) of polymers and of the particle size distribution (PSD) of colloidal (but not only colloidal) particles. A new micro-(μ)-TFFF has recently been developed[3] and its high performance was demonstrated for the separation of the macromolecules in the range of molar mass up to roughly one million g/mol. The possibility of separating the UHMM polymers was previously briefly discussed,[3] but only few experiments demonstrating the fractionation of polystyrene (PS) samples of molar masses 10^6 and 10^7 g/mol were performed.

In this study, the μ-TFFF is applied for high-performance separations of the UHMM polymers. The low heat flux in the μ-TFFF channel allows extending, substantially, the range of perfectly controlled temperature of the cold wall. Such extreme experimental conditions cannot be achieved with the TFFF channels of classical size, due to the difficult evacuation of the high heat energy flux from the cold wall. The variation of the experimental conditions in the μ-TFFF channel, such as the temperature gradient programming and, consequently, the optimization of the time of separation, is very easily realized. Although, this work is devoted mainly to the application of the μ-TFFF for the analysis of the UHMM polymers, an example of the high performance separation and analysis of the colloidal particles is presented.

EXPERIMENTAL

μ-TFFF Equipment

The apparatus for the μ-TFFF consisted of an Intelligent pump Model PU-980 (Jasco, Japan), the injection valve Model 7410 (Rheodyne, USA) equipped

with a 1 μL loop, the UV-VIS variable wavelength Intelligent detector Model UV-975 (Jasco, Japan) with the 1 μL measuring cell, and the recorder–integrator Model HP 3395 (Hewlett-Packard, USA).

The versatile μ-TFFF channel was described in detail in our previous paper.[3] The cold wall temperature was controlled and kept constant during one separation by using a compact, low temperature thermostat Model RML 6 B (Lauda, Germany). The electric power for the heating cartridge was regulated by an electronic variator for both constant and time programmed temperature gradient operations. The temperatures of the cold and hot walls were measured by Digital thermometer (Hanna Instruments, Portugal) equipped with two thermocouples.

Size Exclusion Chromatography

The apparatus for SEC consisted of a L-6000 Merck pump (Hitachi, Ltd., Japan), an injection valve Model 7125 (Rheodyne, USA) equipped with a 20 μL loop, a column of the size 7.8 × 300 mm packed with 9 μm TSK Gel GMHXL, an L-4000 Merck UV-detector (Hitachi, Ltd., Japan), and an integrator D-2500 Chromato-Integrator Merck (Hitachi, Ltd., Japan).

Carrier Liquids

The tetrahydrofuran (THF) for HPLC (Carlo Erba, Italy) was used as a carrier liquid for the μ-TFFF and SEC of PS standards and an aqueous solution of 0.1% detergent Brie 78 (Fluka, Germany) and of 0.02% of NaCl for the μ-TFFF of polymer colloidal particles.

Quasi-Elastic Light Scattering

The PSD and the average particle diameters of all studied samples of colloidal particles were measured by quasi-elastic laser light scattering (QELS), by using model Zetamaster (Malvern Instruments, Ltd., Worcestershire, UK) apparatus.

Polymers and Colloidal Particles

The PS standards of various molar masses (Polysciences, Inc., USA, Knauer, Germany, and Waters Associates, USA) were used as model samples of soluble UHMM polymers. Polystyrene latex (PSL) particles (Duke Scientific Corp., USA) were used as models of nanoparticulate polymer suspensions and

Table 1. Molar Masses of Polystyrene Standards and Particle Sizes of Polymer Latexes

Polystyrene Standard	$M_w \times 10^{-3}$ (g/mol)	$M_n \times 10^{-3}$ (g/mol)	Polydispersity (M_w/M_n)
	Supplier's Data		
PS 115000	115		< 1.04
PS 411000	411	392	1.05
PS 1030000	1,030		< 1.06
PS 10×10^6	10,000		
PS 26×10^6	26,000		
Polymer Latex	**Diameter (nm)**	**Standard Deviation (nm)**	**Chemical Character**
	Supplier's Data		
PSL 60	60 ± 2.5		Polystyrene
PSL 155	155 ± 4		Polystyrene
PSL 343	343 ± 9		Polystyrene
		μ-TFFF data	
PSL 60	61	23	Polystyrene
PSL 155	156	54	Polystyrene
PSL 343	341	75	Polystyrene
PBAL	241	58	Poly-butylacrylate
		QELS data	
PSL 60	63	12	Polystyrene
PSL 155	156	40	Polystyrene
PSL 343	350	80	Polystyrene
PBAL	288	72	Poly-butylacrylate

one polybutylacrylate latex (PBAL), provided kindly by Drs. H. Pasch and T. Ruhl.[4] Molar masses and particle sizes provided by the suppliers and measured by the QELS of the studied samples are given in Table 1.

RESULTS AND DISCUSSION

Micro-TFFF of Ultra-High Molar Mass Polymers at Constant Field Force

The important effect of the concentration of the injected polymer solution was studied previously.[3] In the present study of the UHMM polymers by the

μ-TFFF, the concentrations of the investigated samples were chosen to avoid this effect on the results of the fractionation. We have discussed, previously,[3] the papers,[5–9] concerning the TFFF of the UHMM polymers. The inverted elution order of the UHMM PS at high flow rates ($\langle v \rangle = 2.68$ cm/sec) was observed by Giddings et al.[6] On the other hand, Chubarova and Nesterov[8] interpreted some of their results as a proof of the shear degradation of the UHMM PS under the conditions of the experiments. Although, Janca and Martin,[7] in a detailed study of the TFFF of the UHMM PS under various experimental conditions, did not confirm the shear induced focusing effect that might explain the mentioned inverted elution order nor the attribution of early eluted peaks to the products of shear degradation, the operational conditions of the μ-TFFF in this study were chosen to avoid the possibility that the results of the fractionations are influenced either by the focusing effect or by the shear degradation. The retention order of the UHMM PS obtained previously[3] at low flow rates, confirmed the normal, polarization mechanism of the separation and very good reproducibility of the experiments.

Figure 1 summarizes the results of the study of the retention of the PS within the range of the molar masses from 1.15×10^5 to 26×10^6 g/mol, at different constant temperature differences between the hot and cold wall and at roughly the same temperature of the cold wall. At the highest temperature gradient $\Delta T = 40$K (Fig. 1a), the lowest molar mass PS is well retained and separated from the void volume, V_0, of the marker peak. On the other hand, the retentions of the PS samples of the molar masses over one million g/mol were found as too high. For the temperature gradient $\Delta T = 20$K (Fig. 1b), the separation is good within the molar mass range from 1×10^6 to 10×10^6 g/mol. The retentions are too low or high below and above this range, respectively. At $\Delta T = 10$K, the retention and fractionation is good for the molar mass 10×10^6 g/mol and higher (Fig. 1c), but the separation of the void volume marker peak and of the PS of molar mass 1.03×10^6 g/mol is not sufficient. At the lowest temperature gradient $\Delta T = 5$K, (Fig. 1d), even the highest molar mass PS is not well resolved from the void volume peak. The frontal shoulder of the void volume peak on the fractogram of the PS 10×10^6, indicates that a small part of the macromolecules was not relaxed sufficiently. This part of the macromolecules, which has not enough time (just after the injection into the channel) to establish a steady-state concentration distribution across the channel, is eluted more rapidly (in average) compared with the macromolecules exerting a steady-state concentration distribution during their whole course inside the channel.

The resulting fractograms, thus, represents an overlay of the accurate separation of the species according to their size by an imperfect separation of the species not exerting the steady-state concentration distribution from the very beginning of the fractionation. Definite experimental proof that the frontal

MARCEL DEKKER, INC. • 270 MADISON AVENUE • NEW YORK, NY 10016

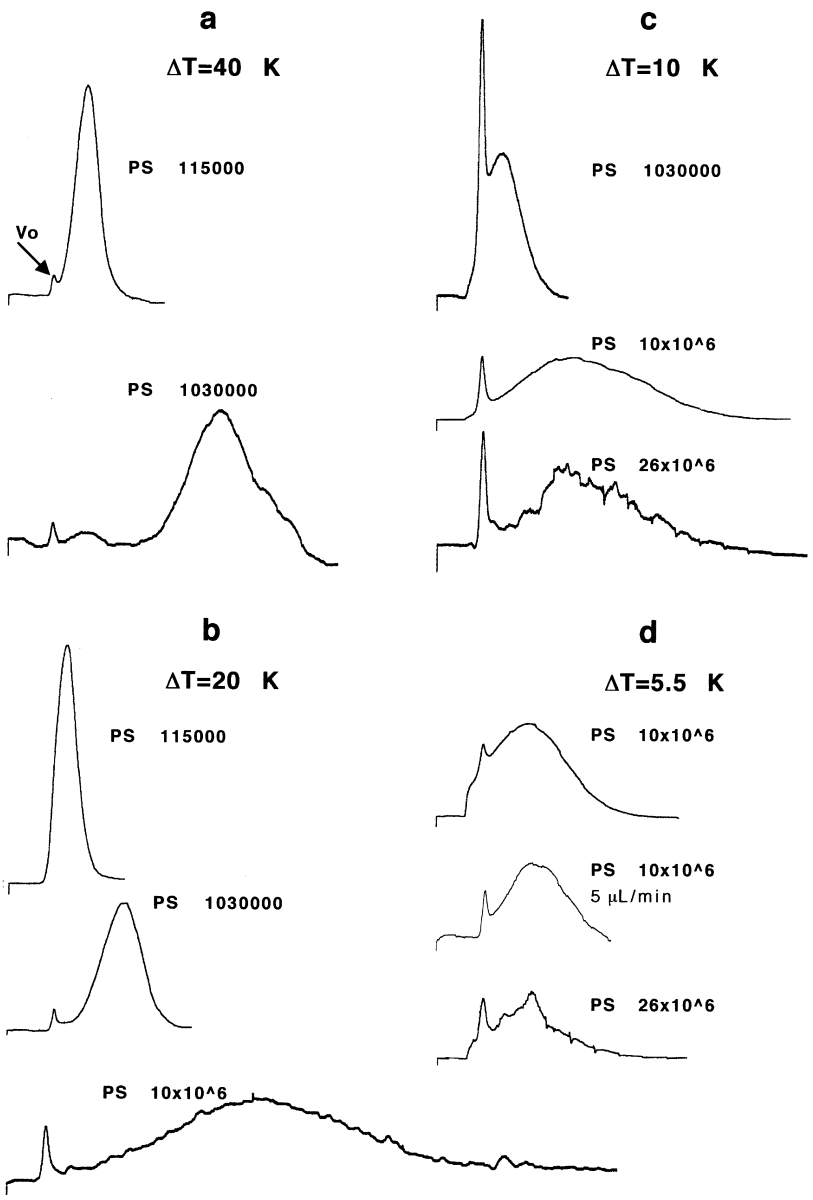

Figure 1. Fractograms of the individual UHMM PS samples obtained by μ-TFFF at different temperature gradients ΔT. Experimental conditions: flow-rate 20 μL/min; temperatures of the cold wall, $T = 18°C$ for $\Delta T = 40K$, $T = 17°C$ for $\Delta T = 20K$, $T = 16°C$ for $\Delta T = 10K$, and $T = 15.5°C$ for $\Delta T = 5.5K$, injected volume 1 μL.

shoulder (or even a separate frontal peak eluting before the void volume V_0) corresponds well to the species not enough relaxed (and not to some fraction of the degraded macromolecules) was given previously.[3,7] The frontal shoulder disappears at lower flow rate of 5 μL/min (Fig. 1d).

With regard to these results, two problems are obvious. The first is related to the width of the fractograms, which increases with the increasing molar mass but it is not clear whether the width of larger fractograms corresponds to a broader MMD or to a lower efficiency of the separation. The concentration-viscosity effects, known in SEC,[10] cannot explain this observation because, as mentioned above, the concentrations of the injected solutions were optimized to suppress these effects. The second problem is that the operation with constant temperature gradient does not allow fractionation of a more extended range of molar masses in one experiment, and in a reasonable time.

The answer to the first problem was found by a comparative study of the same PS samples by the SEC. The results are represented in Fig. 2, which shows that the width of the particular peaks actually increases with the molar mass. The SEC chromatograms shown in Fig. 2, were obtained at low concentrations and their widths did not decrease further for still lower concentrations. It means that only the polydispersity in MMD, and not the concentration–viscosity effects, can explain the increase of the peak width with increasing molar mass. The calibration curve of the SEC column in Fig. 3 shows that the selectivity of the column is relatively good even for the UHMM PS. As a result, relatively large μ-TFFF fractograms correspond well to broader MMD of the samples in question (in agreement with the SEC chromatograms in Fig. 2 and with the data in Table 1) and not to a lower efficiency of the μ-TFFF separation system.

A convenient solution of the second problem concerning the extension of the molar mass range covered by a single experiment and carried out in a reasonable time, is to apply a programmed decrease of the temperature gradient in the course of the fractionation. The programmed operation was studied and is described in this paper.

Resolution in μ-TFFF and SEC

In order to demonstrate the resolution, which can be attained with the μ-TFFF system, a mixture of three PS's was fractionated. The result is shown in Fig. 4. As the temperature gradient in this experiment, $\Delta T = 22$K, was slightly different compared with the experiments shown in Fig. 1; the fractogram of each particular PS component of the mixture is shown in Fig. 4, together with the fractogram of the mixture obtained under identical experimental conditions. The same samples were fractionated by the SEC and the resulting chromatograms are

MARCEL DEKKER, INC. • 270 MADISON AVENUE • NEW YORK, NY 10016

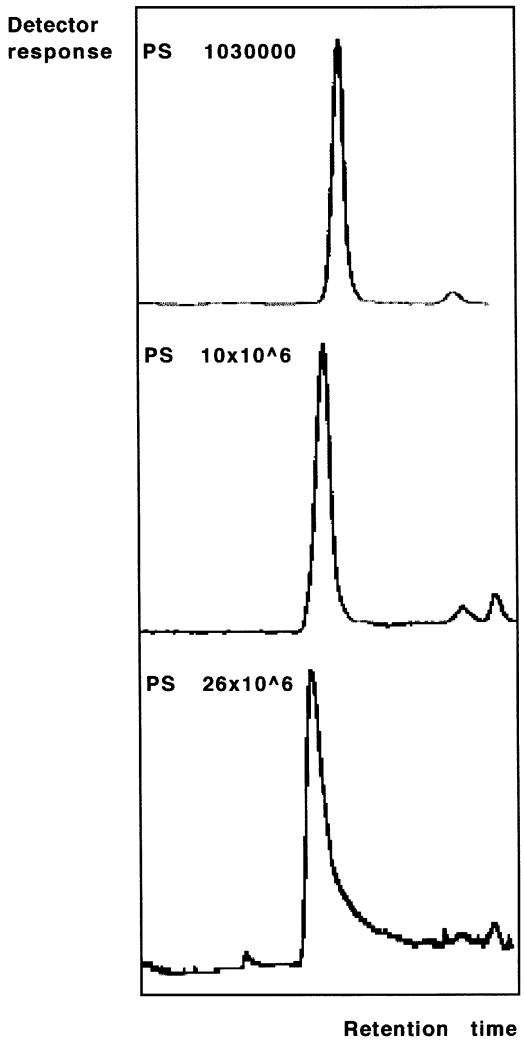

Figure 2. SEC chromatograms of the individual UHMM PS samples. Experimental conditions: flow-rate 1 mL/min, injected volume 20 μL.

also shown for comparison in Fig. 4. A qualitative conclusion that can be drawn from the μ-TFFF fractograms and SEC chromatograms is that the resolution of the peaks corresponding to the PS of molar masses 115×10^3 and 1.03×10^6 g/mol is similar for both methods, for about the same time of analysis

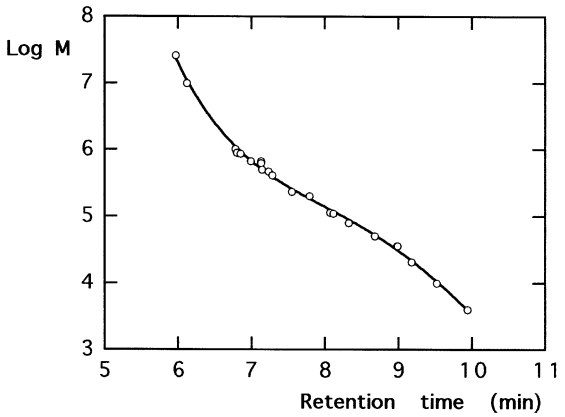

Figure 3. Calibration curve of the SEC column obtained under the experimental conditions given in Fig. 2.

of ca. 15 min. It is impossible to evaluate the resolution for the PS of 1.03×10^6 and 10×10^6 g/mol because the MMD of these samples are overlapping.

Further increase of the resolution of the μ-TFFF, as well as of the SEC, is possible by decreasing the flow rate. Theoretically, such a variation of the flow rate should lead to a similar increase of the resolution for both methods. However, more efficient increase of the resolution in μ-TFFF can be achieved by increasing the temperature gradient and, consequently, the retention. It has been shown in our recent paper,[3] that a high resolution comparable with that for the PS 115×10^3 and 1.03×10^6 g/mol shown in Fig. 4, was obtained for the PS 115×10^3 and 411×10^3 g/mol at $\Delta T = 40$K. Obviously, such versatility in manipulating the resolution is not available in SEC. The superposition of the SEC chromatograms of individually injected samples in Fig. 4 indicates that the resolution between the PS 115×10^3 and 411×10^3 g/mol achieved previously[3] in μ-TFFF at $\Delta T = 40$K is out of performance of the SEC, as proven by the injection of the mixture (Fig. 4).

The above evaluation of the resolution in the μ-TFFF and SEC of the UHMM PS is based only on a visual comparison of the fractograms and chromatograms. A long time ago, a similar approach has been used in the first comparison of the performance of standard size TFFF channel with SEC.[11] However, a more accurate comparison of the μ-TFFF with modern SEC can be obtained by calculating the average molar masses M_w and M_n and the corresponding polydispersity indexes M_w/M_n for individually retained samples, without applying any correction for band broadening. Such a comparison eliminates all problems of overlapping peaks. A relevant study is in progress.

MARCEL DEKKER, INC. • 270 MADISON AVENUE • NEW YORK, NY 10016

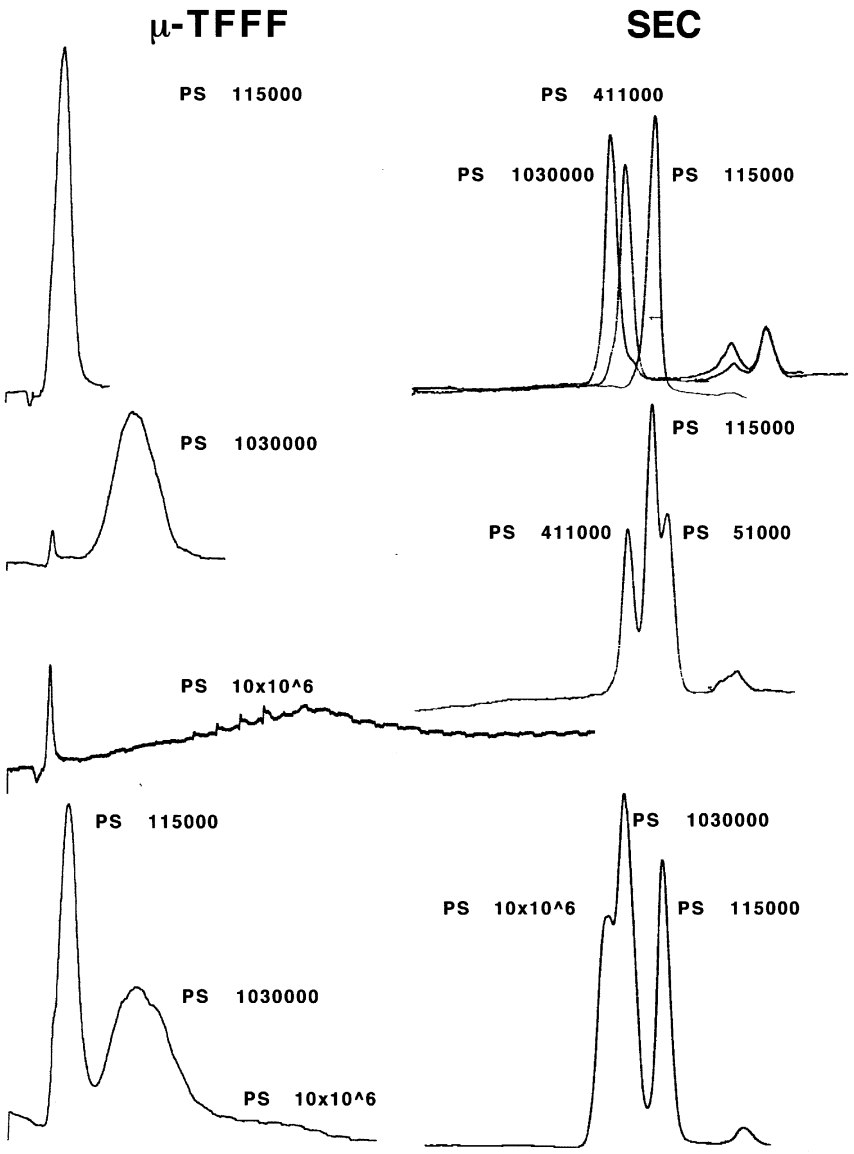

Figure 4. Micro-TFFF fractograms of the individual UHMM PS samples and of their mixture and the SEC chromatograms of the individual UHMM PS samples and of the same mixture as that fractionated by the μ-TFFF. Experimental conditions: μ-TFFF, flow-rate 10 μL/min; temperature of the cold wall, $T = 17°C$ with $\Delta T = 21$ K; SEC, given in Fig. 2.

Programming of the Temperature Gradient in μ-TFFF

The general concepts of the field force programming were proposed at early stages of the field-flow fractionation development.[12] A parabolic decrease of the temperature gradient ΔT in time was proposed by Giddings et al.[13] and a very advantageous exponential course of the program in TFFF by Kirkland and Yau.[14] The following applications of the temperature gradient programming in TFFF were not very numerous.[15–17]

The particular functions (parabolic, exponential, etc.) were imposed previously on the course of the temperature gradient decrease, in order to keep a relationship between a chosen retention parameter (e.g., retention time or retention ratio R) and a molecular characteristic of the retained species (e.g., molar mass or size) as smooth as possible, preferentially linear. While the smoothness of such a relationship is a reasonable condition in order to avoid the appearance of possible artifacts on the fractograms, if the variation of the temperature gradient would be too abrupt, the relationship should not be linear. Similar tendencies were observed in tailoring the SEC columns characteristics but, as a matter of fact, the importance of such a linear property of a separation system is rather in the commercial publicity than in the performance. By taking into account all imperfections of real fractograms due to the noise of the signal of a detector, drift of the base-line, etc., which became more and more important when pushing down the lower limits of the amount of the analyzed samples, but which can easily be corrected almost on-line by powerful computer techniques, the treatment of the experimental data, which are not linear, does not represent an additional problem at all.

The introduction of the μ-TFFF, however, represents a problem to be solved when operating with the time-programmed temperature gradient. While the decrease of the temperature gradient in standard size TFFF is relatively slow because the whole separation run can last hours and, consequently, heat capacity and thermal conductivity of the material used for the construction of the channel is not very important, the thermal inertia of the channel for the μ-TFFF, with all its necessary elements for efficient heating, cooling, and temperature control, is an important factor to be considered when the use of a time-programmed field force is intended.

We have studied, in detail, the above mentioned problems related to the time-programmed field force operation with the μ-TFFF. Few convenient shapes of the programmed decrease of the temperature gradient, achieved on our μ-TFFF channel, are shown in Fig. 5. The results of the successful fractionations of the PS UHMM standards by using the time-programmed decrease of the temperature gradient, are shown in Fig. 6. In the first case, in Fig. 6a, the fractogram **1** of the PS of molar mass 1.03×10^6 g/mol was obtained at $\Delta T = 40$K, constant during the whole run. The fractogram **2** in Fig. 6a was obtained with temperature

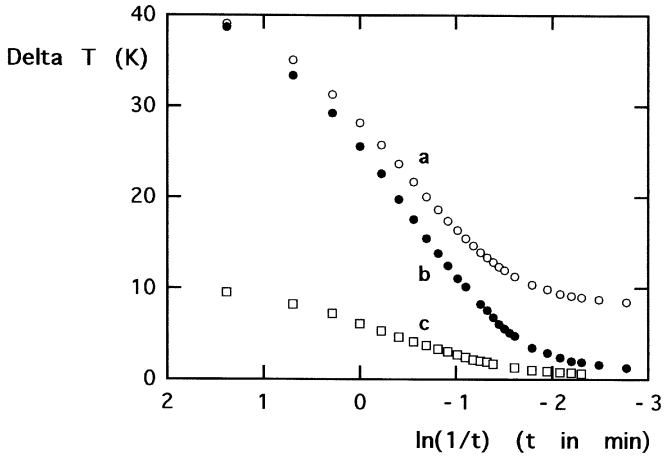

Figure 5. Course of various typical time programs of the temperature gradient decrease on the μ-TFFF channel.

gradient decreasing from $\Delta T = 40$K to $\Delta T = 0$K, according to the program represented by the curve b in Fig. 5, which started after 8 min of constant $\Delta T = 40$K; and, finally, the fractogram **3** was obtained with the same program, which started sooner after 5 min of constant $\Delta T = 40$K. Although, the PS of the molar mass 1.03×10^6 g/mol is fractionated at constant $\Delta T = 40$K in a reasonable time, and well separated from the void volume peak, both runs with temperature gradient program represent an important shortening of the time of fractionation. On the other hand, the PS of the molar mass 10×10^6 g/mol was fully retained at constant $\Delta T = 40$K (not shown in Fig. 6b). The programmed decrease of the temperature gradient was necessary to obtain the correct fractograms shown in Fig. 6b. The fractogram **1** in Fig. 6b was obtained by applying the temperature gradient decrease corresponding to the curve b in Fig. 5, started after 26 min of constant $\Delta T = 40$K. The fractogram **2** was obtained by applying the same temperature gradient decrease, but started only after 8 min of constant $\Delta T = 40$K. At last, the fractogram **3** was obtained by applying the temperature gradient decrease corresponding to the curve a in Fig. 5, started after 8 min of constant $\Delta T = 40$K and finished with stabilized $\Delta T = 10$K. In principle, all three programs applied for the μ-TFFF of the PS sample of molar mass 10×10^6 g/mol resulted in an efficient fractionation.

A crucial test of the performance of the μ-TFFF with time-programmed decrease of the temperature gradient, was provided by a separation of model mixture of three PSs of the molar masses 115×10^3, 1.03×10^6, and 10×10^6 g/mol. The corresponding fractogram is shown in Fig. 7. The fractogram

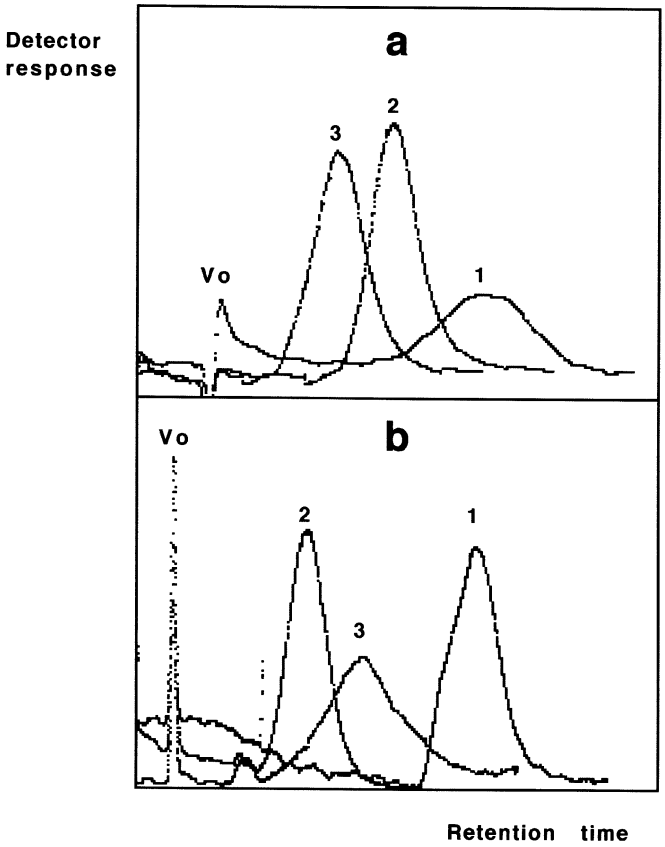

Figure 6. Fractograms of the individual UHMM PS samples obtained by the μ-TFFF at constant temperature gradient ΔT and with various time programs of the temperature gradient decrease. (a) PS sample of molar mass 1.03×10^6 g/mol, experimental conditions: flow-rate 20 μL/min, temperature of the cold wall, $T = 18°C$ for $\Delta T = 40K$, and $T = 15°C$ for $\Delta T = 0K$, injected volume 1 μL. Fractogram **1**, constant $\Delta T = 40K$ during the whole separation run; fractogram **2**, program started after 8 min of constant $\Delta T = 40K$, final $\Delta T = 0K$; fractogram **3**, program started after 5 min of constant $\Delta T = 40K$, final $\Delta T = 0K$. (b) PS sample of molar mass 10×10^6 g/mol, experimental conditions: flow-rate 20 μL/min, temperature of the cold wall, $T = 18°C$ for $\Delta T = 40K$, and $T = 16°C$ for $\Delta T = 10K$, injected volume 1 μL. Fractogram **1**, program started after 26 min of constant $\Delta T = 40K$, final $\Delta T = 0K$; fractogram **2**, program started after 8 min of constant $\Delta T = 40K$, final $\Delta T = 0K$; fractogram **3**, program started after 8 min of constant $\Delta T = 40K$, final $\Delta T = 10K$.

MARCEL DEKKER, INC. • 270 MADISON AVENUE • NEW YORK, NY 10016

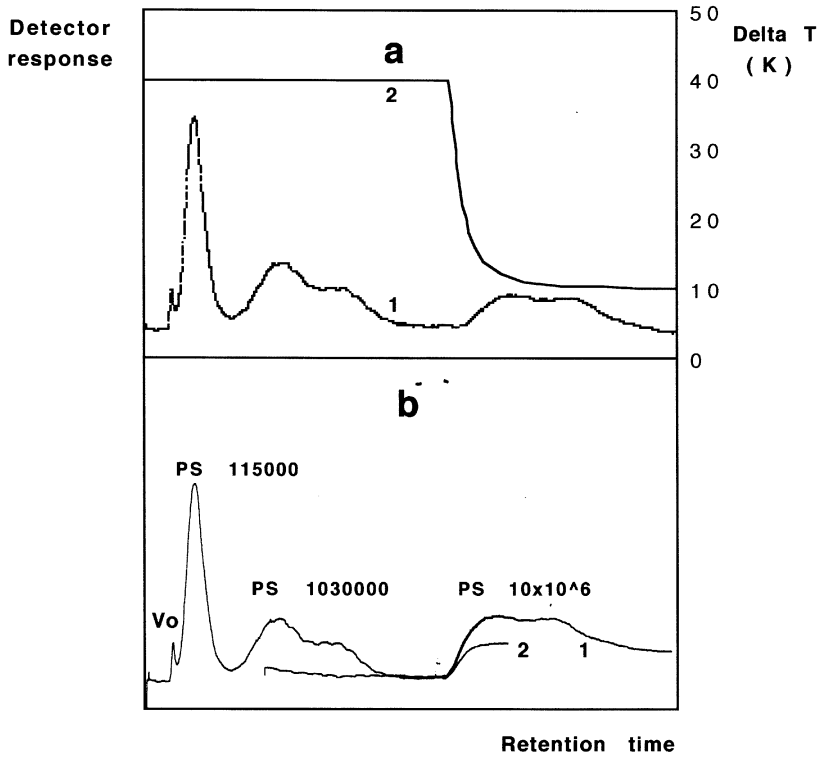

Figure 7. Fractogram of the mixture of UHMM PS samples obtained by the μ-TFFF with time-programmed decrease of the temperature gradient. (a) Fractogram corrected for the shift of the base-line (curve **1**) and the course of the temperature gradient decrease during the fractionation run (curve **2**). (b) Raw μ-TFFF fractogram (curve **1**) and the base-line shift (curve **2**) obtained by applying the relevant program of the decrease of temperature gradient without injecting the PS sample. Experimental conditions: flow-rate 20 μL/min, cold wall temperature, $T = 18°C$ for $\Delta T = 40K$, and $T = 16°C$ for $\Delta T = 10K$, injected volume 1 μL.

corrected for the shift of the baseline is shown in Fig. 7a, together with the course of the programmed decrease of the temperature gradient (curve **2** in Fig. 7a). The comparison of this fractogram with those for the individual components of the mixture obtained at different but constant temperature gradients, shown in Fig. 1, and with the fractogram of the identical mixture obtained at lower but constant temperature gradient, shown in Fig. 4, indicates clearly the gain in resolutions concerning all components of the mixture fractionated in programmed field force mode. The mentioned correction for the shift of the baseline is explained in Fig.

7b, which shows the raw fractogram (curve **1** in Fig. 7b) overlaid by the detector response recorded in a separate experiment without the injection of the sample, but with the application of the same programmed decrease of the temperature gradient as in the fractionation experiment (curve **2** in Fig. 7b). The observed baseline shift is very reproducible with the same programming protocol, which makes the correction feasible.

Micro-TFFF of Colloidal Particles

In the last few years, the TFFF became quite popular for the separation and characterization of colloidal particles.[18–29] The theoretical and experimental studies indicate that the size (or mass) of the particles, as well as their surface properties and, consequently, the interactions between the particles and the components of the carrier liquid, determine the amplitude of the thermal diffusion coefficient. The retention then depends on the ratio of the thermal diffusion to ordinary Fickian (Brownian) diffusion coefficients. With regard to the size of the colloidal particles, their diffusion coefficients are very low. Consequently, a low temperature gradient can generate an important retention. Whenever the temperature gradient is relatively high, all particles can be compressed to the accumulation wall of the channel independently of their size and surface properties. In such a case, the steric exclusion mechanism dominates the separation, and the elution order is from the largest to the smallest particles.

On the other hand, at high flow rates, the hydrodynamic lift forces can play an important role and complicate the separation due to the action of a focusing mechanism. Obviously, the mechanism of separation can become quite complex. However, if the intervention of various contributing forces is mastered, both theoretically and experimentally, the TFFF can offer extensive possibilities to characterize various physico-chemical parameters and properties of the colloidal particles.

The intention of this part of our investigation was to verify whether the performance of the μ-TFFF channel is sufficient, in agreement with the theoretical assumptions, to be utilized in more extensive and detailed further studies of this new technique for the separation and analysis of the colloidal particles.

The results of the experimental study are shown in Fig. 8. Figure 8a represents the μ-TFFF fractograms of the PSL of different average particle sizes, obtained under identical experimental conditions with constant temperature gradient applied. These fractograms, and the supplier's data, were used to construct a calibration curve, which served to calculate the average particle sizes and standard deviations of the PSD of these PSL samples, as well as of the "unknown" sample of PBAL. All these data, given in Table 1, demonstrate good

MARCEL DEKKER, INC. • 270 MADISON AVENUE • NEW YORK, NY 10016

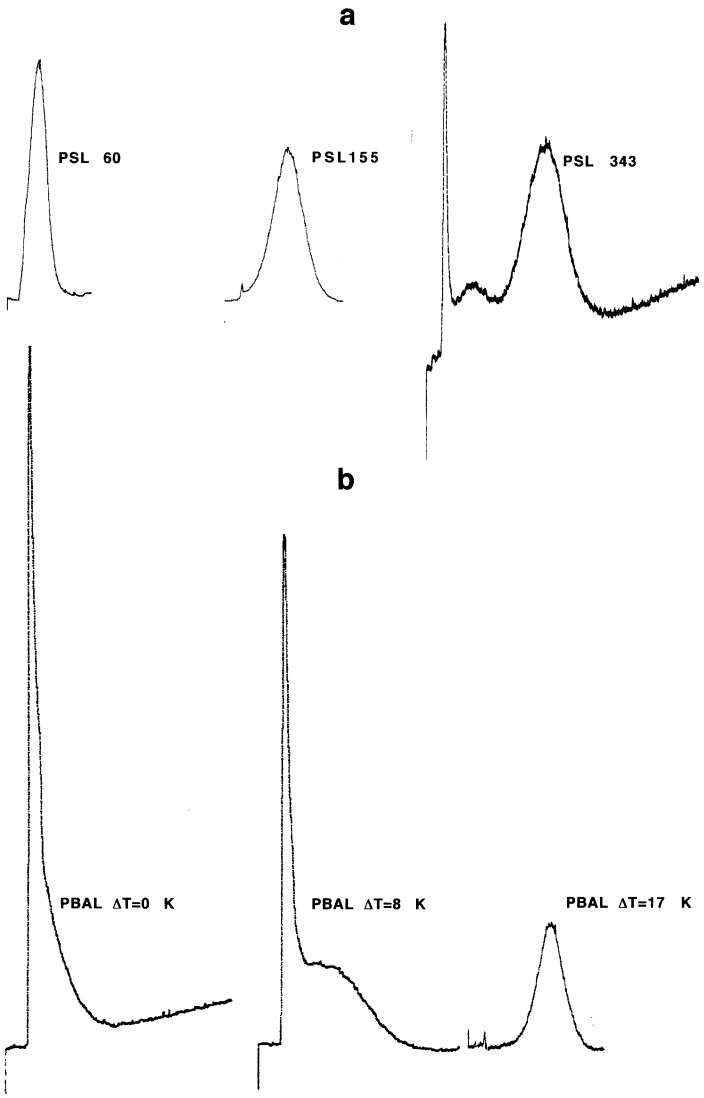

Figure 8. Fractograms of the individual colloidal particles samples obtained by the μ-TFFF at constant temperature gradient ΔT. (a) Fractograms of different size PSL particles. Experimental conditions: flow-rate 10 μL/min, cold wall temperature, $T = 18°C$ for $\Delta T = 18K$, injected volume 1 μL. (b) Fractograms of the PBAL sample of colloidal particles obtained at different constant temperature gradients. Experimental conditions: flow-rate 20 μL/min, cold wall temperature, $T = 15°C$ for $\Delta T = 0K$, $T = 17°C$ for $\Delta T = 8K$, $T = 19°C$ for $\Delta T = 17K$, injected volume 1 μL.

agreement of our μ-TFFF results with the results of the QELS measurements, as well as with the data of supplier.

The μ-TFFF fractograms in Fig. 8b represent the evolution of the zone of the PBAL sample from the unretained, obtained at $\Delta T = 0$K, until the well retained zone at $\Delta T = 17$K, and passing through a partially retained zone at $\Delta T = 8$K. One can see the progressive disappearance of a part of the unrelaxed particles, which are still present as separate peak on the fractogram at $\Delta T = 8$K, but completely disappearing on the fractogram obtained at $\Delta T = 17$K. We have not studied, in this part of our work, the positive effect of the stop-flow procedure during the initial relaxation period, which certainly could lead to obtaining the accurate results in a shorter time, even if the total fractionation time, 50 min of the μ-TFFF carried out under conditions resulting in high performance fractionation of the PBAL sample at the temperature gradient $\Delta T = 17$K, is not at all bad. Our extended study of the μ-TFFF of the colloidal particles of different chemical nature, within more extended ranges of their sizes and including a detailed investigation of the relaxation phenomena, is in progress.

CONCLUSIONS

The application of the μ-TFFF for the separation of UHMM polymers, confirmed the performance of this new technique, which is higher than that obtained with classical size channels, in agreement with the theoretical predictions. A qualitative comparison of the resolution achieved in the domain of the UHMM PS by using the μ-TFFF with the resolution obtained with an SEC column, provided the results in favor of the μ-TFFF, even if the whole potential of the μ-TFFF to further increase the resolution was not yet exploited on its far limits.

The time-programming of a decrease of the temperature gradient during the fractionation run, proved the efficiency of this operational mode, especially for the UHMM polymers. The application of this technique leads to a substantial shortening of the analysis time by keeping high the performance of the fractionation.

Although, not yet optimized in several operational parameters and experimental conditions, the μ-TFFF of the colloidal particles is a promising technique. The potential of the high-performance μ-TFFF in the separation, analysis, and characterization of not only the synthetic or inorganic colloidal particles, but also of the particles of biological origin, can be very useful. The most important advantages of the μ-TFFF applied in this field, are the possibility of coupling this high performance separation technique with highly selective detection systems such as mass spectroscopy and others, substantially enlarged

domain of the temperature, at which the channel for the μ-TFFF can work and a reduced sample amount, only few nanograms, needed for the analysis.

REFERENCES

1. Janca, J. *Field-Flow Fractionation: Analysis of Macromolecules and Particles*; Marcel Dekker, Inc.: New York, 1988.
2. Schimpf, M.E.; Caldwell, K.D.; Giddings, J.C. *Field-Flow Fractionation Handbook*; John Wiley & Sons: New York, 2000.
3. Janca, J. J. Liq. Chromatogr. & Rel. Technol. *in press.*
4. Ruhl, T.; Pasch, H. Deutsches Kunststoff-Institut, Darmstadt, Germany.
5. Gao, Y.S.; Caldwell, K.D.; Myers, M.N.; Giddings, J.C. Macromolecules **1985**, *18*, 1272.
6. Giddings, J.C.; Li, S.; Williams, P.S.; Schimpf, M.E. Makromol. Chem., Rapid Commun. **1988**, *9*, 817.
7. Janca, J.; Martin, M. Chromatografia **1992**, *34*, 125.
8. Chubarova, E.V.; Nesterov, V.V. In *Strategies in Size Exclusion Chromatography*, ACS Symposium Ser.; Potschka, M., Dubin, P.L., Eds.; Am. Chem. Soc.: Washington, D.C., 1996; 635, 127 pp.
9. Lee, S.; Kwon, O.S. In *Chromatographic Characterization of Polymers, Hyphenated and Multidimensional Techniques*, ACS Symposium Ser.; Provder, T., Barth, H.G., Urban, M.W., Eds.; Am. Chem. Soc.: Washington, D.C., 1995; 247, 93 pp.
10. Mori, S. In *Steric Exclusion Liquid Chromatography of Polymers*; Janca, J., Ed.; Marcel Dekker, Inc.: New York, 1984.
11. Giddings, J.C.; Yoon, Y.H.; Myers, M. Anal. Chem. **1975**, *47*, 126.
12. Grushka, E.; Caldwell, K.D.; Myers, M.N; Giddings, J.C. In *Separation and Purification Methods*; Perry, E.S., Van Oss, C.J., Grushka, E., Eds.; Marcel Dekker, Inc.: New York, 1973; Vol. 2.
13. Giddings, J.C.; Smith, L.K.; Myers, M.N. Anal. Chem. **1976**, *48*, 1857.
14. Kirkland, J.J.; Yau, W.W. Macromolecules **1985**, *18*, 2305.
15. Kirkland, J.J.; Rementer, S.W.; Yau, W.W. Anal. Chem. **1988**, *60*, 610.
16. Giddings, J.C.; Kumar, V.; Williams, P.S.; Myers, M.N. In *Polymer Characterization*, ACS Advances in Chemistry Series; Craver, C.D., Provder, T., Eds.; ACS: Washington, D.C., 1990; 227 pp.
17. Williams, P.S.; Giddings, J.C. J. Chromatogr. **1991**, *550*, 787.
18. Liu, G.; Giddings, J.C. Anal. Chem. **1991**, *63*, 296.
19. Liu, G.; Giddings, J.C. Chromatographia **1992**, *34*, 483.
20. Shiundu, P.M.; Liu, G.; Giddings, J.C. Anal. Chem. **1995**, *67*, 2705.
21. Shiundu, P.M.; Giddings, J.C. J. Chromatogr. **1995**, *715*, 117.

22. Ratanathanawongs, S.K.; Shiundu, P.M.; Giddings, J.C. Colloids Surf. A: Physicochem. Eng. Aspects **1995**, *105*, 243.
23. Giddings, J.C.; Shiundu, P.M.; Semenov, S.N. J. Colloid Interface Sci. **1995**, *176*, 454.
24. Jeon, S.J.; Schimpf, M.E. Polym. Mater. Sci. Eng. **1996**, *75*, 4.
25. Van Batten, C.; Hoyos, M.; Martin, M. Chromatographia **1997**, *45*, 121.
26. Jeon, S.J.; Schimpf, M.E.; Nyborg, A. Anal. Chem. **1997**, *69*, 3442.
27. Semenov, S.N. J. Microcolumn Sep. **1997**, *9*, 287.
28. Semenov, S.N. J. Liq. Chromatogr. & Rel. Technol. **1997**, *20*, 2687.
29. Mes, E.P.C.; Tijssen, R.; Kok, W.Th. J. Chromatogr. A **2001**, *907*, 201.

Received February 24, 2002
Accepted March 12, 2002
Manuscript 5792